Geomorphology 117 (2010) 121–129

Contents lists available at ScienceDirect

Geomorphology

journal homepage: www.elsevier.com/locate/geomorph

Regional-scale relief evolution and large landslides: Insights from geomechanical analyses in the Tinée Valley (southern French Alps)

Yves Guglielmi [a], Frédéric Cappa [b,*]

[a] Géologie des Systèmes et des Réservoirs Carbonatés, University of Provence Aix-Marseille, France
[b] GeoAzur (UMR6526), University of Nice Sophia-Antipolis, Côte d'Azur Observatory, Sophia-Antipolis, France

ARTICLE INFO

Article history:
Received 8 October 2009
Received in revised form 29 October 2009
Accepted 14 November 2009
Available online 22 November 2009

Keywords:
Landslides
Failure
Rock mass strength
Chronology
Numerical simulations
Argentera–Mercantour massif

ABSTRACT

Recurring large rock-slope failures of the Argentera–Mercantour massif (southern French Alps) over the past 20,000 years were identified in the field and analyzed using a continuum mechanics approach based on material weakening in a three-dimensional finite-difference model. We compared a mountain-slope failure model neglecting the effect of rock strength loss with a model simulating the effect of strength loss and integrating cohesional weakening and frictional strengthening processes. The good correspondence between the relative chronology and location of observed and simulated deformations shows that (1) the gradual loss of rock mass strength related to stress release effects following the Pleistocene deglaciation can be as long as several thousands of years, and (2) the causes and triggering of the present-day active landslides are related to this long failure history. Our study suggests that the episodic nature of massive rock slides can be explained through the gradual development of tensile and shear failure, and time-dependent strength degradation. Our numerical model is a good reproduction of large landslides at the regional-scale of a mountainous massif.

1. Introduction

In geodynamical processes of mountain relief evolution, landslides play an efficient role in hillslope adjustments to tectonic and climatic forcing (Jarman, 2006). Under high rates of rock uplift and erosion, hillslope topography attains a critical inclination and height that is controlled by material strength loss, effective stress redistribution, and changes in geometry and boundary conditions with time. From an engineering geology perspective, approaches conventionally used to model rock-slope failure involve discontinuum models based on fracture mechanics or continuum models based on material weakening. In most cases, models explore factors contributing to rock-slope failure at the slope-scale and with a limited consideration of time evolution of processes. Main results of these studies are that landslides either occur in the steepest slopes or that extensive weak low angle discontinuities favour large destabilisations in all kinds of slope topography.

One major scientific challenge remains in understanding processes involved in deep-seated deformations, their possible links to giant catastrophic landslides and to actual landslides (Agliardi et al., 2001; Ballantyne, 2002). Deep-seated deformations are observed in all mountain ranges and in all kinds of geological context: deformations also called "sackung" (Zischinsky, 1966), mass rock creep, depth creep, deep-seated creep, gravitational spreading, and deep-seated gravitational slope deformation (DSGSD; Dramis and Sorriso-Valvo, 1994). DSGSD are regional-scale destabilized volumes characterized by a very long time evolution spreading over thousands of years (Brückl and Parotidis, 2005; Petley et al., 2005). Recent papers show that DSGSD can be precursors of catastrophic landslides (Brückl and Parotidis, 2005). One other major difference between DSGSD and landslides is that DSGSD appear more like a diffuse deformation in the mountain volume while large landslides are bounded by a clear failure surface. This could mean that, as it was reproduced at the laboratory scale (Martin and Chandler, 1994; Hajiabdolmajid et al., 2002), failure is progressively initiating at the regional-scale and then propagating at the slope-scale.

Nevertheless, there are very few models looking at the DSGSD processes at the regional-scale down to the landslide local slope-scale. Three-dimensional failure propagation reproduced in physical models using an analogue material (Bachmann et al., 2004; Chemenda et al., 2005; Bachmann et al., 2006, 2008) show that high relief induces large-scale (large volume) gravitational movements. Introduction of small-scale topographic features results not only in the generation of smaller-scale landslides, but also in considerable changes in the deformation pattern. The various-scale processes occur simultaneously and affect each other. To predict the evolution of a landslide, it is therefore necessary to take into account the topography and deformation pattern at various scales. Generally, material strength in numerical models are based on a linear Mohr–Coulomb or a non-linear Hoek–Brown failure criterion, assuming that both the cohesional and frictional components of strength in the intact and fractured portions of rocks contribute to peak strength, and are simultaneously modified (Hajiabdolmajid et al., 2002). The simultaneous changes of cohesive and frictional strength components are considered valid at high stress levels, when the rock

* Corresponding author. Fax: +33 4 92 94 26 10.
E-mail addresses: yves.guglielmi@univ-provence.fr (Y. Guglielmi), cappa@geoazur.unice.fr (F. Cappa).

0169-555X/$ – see front matter © 2009 Elsevier B.V. All rights reserved.
doi:10.1016/j.geomorph.2009.11.016

behaves in a ductile manner (Mogi, 1966; Amitrano, 2003), and cohesion and friction can be modified simultaneously. However, in the case of brittle rocks in a compressive stress field at low confinement, Martin et al. (1999) argue that the assumption of instantaneous and simultaneous changes in cohesion and friction is not correct because under these conditions, cracks dilate or open after initiation, inhibiting coincidental variations of friction and cohesion. This conclusion is supported by laboratory studies that suggest that brittle strength variations can be reasonably represented as a two-stage process: (1) a pre-peak behaviour dominated by the cohesive strength of the rock, and (2) a residual strength controlled by the changes in frictional strength within the damaged rock (Martin and Chandler, 1994; Hajiabdolmajid et al., 2002). Thus, at low confinement levels, frictional strength cannot be modified until the rock is sufficiently damaged to become essentially cohesionless.

In nature, failure of rock slopes generally occurs in low stress environments (few MPa), with a gradual failure sequence including complex interactions between pre-existing discontinuities and fracture propagation through intact rock bridges (Kemeny, 2003; Eberhardt et al., 2005; Kemeny, 2005). Strength components are not simultaneously and fully modified during damage because failure primarily occurs in rock bridges between discontinuities by tensile fracturing (Diederichs, 1999) that first induces a cohesion loss before the friction can contribute to the changes in strength (Hajiabdolmajid and Kaiser, 2002). Thus, conventional modelling approaches ignoring material weakening or assuming simultaneous changes in strength parameters either overestimate (when cohesion is set to 0) or underestimate (when simultaneous variations of cohesion and friction are considered) the altered strength in the failure process.

Many studies have reported that rock failure involves the initiation, growth and accumulation of cracks (Eberhardt et al., 1999; Hajiabdolmajid et al., 2002). They have shown that modelling approaches based on traditional failure criteria and strain-softening models have not been successful in predicting the depth and failure extent of rocks at low confinement levels. To improve models that progressively bring rocks to failure, Hajiabdolmajid et al. (2002) proposed a cohesion weakening–frictional strengthening (CWFS) model for simulating failure when using a continuum modelling approach with conventional failure criteria. This model considers cohesion loss and friction increase as a function of plastic strain.

In the study presented here, we used the CWFS model to numerically simulate the effects of gravity loading on the initiation of failure in rock slopes of a mountainous massif. We applied the CWFS model to the Argentera–Mercantour massif in the southern French Alps, a region especially prone to slope movement, ranging in magnitude from small rockfalls to extensive gravitational deformations involving several tens of millions of cubic metres of rock (Guglielmi et al., 2004). The massif is cut by two valleys, the Tinée and the Stura valleys, which show several gravitational deformations of different ages from the valley floors to the mountain crests. Large rockslides (volumes exceeding 5×10^6 m^3) are characterized by failure surfaces at the toes of hillslopes and several kilometres of long tension cracks on the upper hillslopes. These currently active mass movements are situated in a formerly glaciated mountainous massif, and currently under temperate climate and moderate seismicity (Cappa et al., 2004; Guglielmi et al., 2005). Through our investigations, we estimated how a continuum modelling approach with cohesion loss and frictional strength increase (CWFS) at a regional-scale can reproduce the gravity-driven failure sequences in rock slopes of a mountainous valley.

2. Regional inventory of landslides in the Argentera–Mercantour massif

The metamorphic gneissic basement of the Argentera–Mercantour massif (Fig. 1) has a pervasive foliation striking N150–60°E, and it is cut by three sets of near-vertical faults striking N010°E–N030°E, N080°E–N090°E and N110°E–N140°E. The metamorphic rocks are weathered to a depth of 50 to 200 m. Weathering is characterized by an increase in fracture density, a toppled foliation that dips less than 20° to the NE or SW, and chemical alteration of minerals to clay (Cappa et al., 2004; Guglielmi et al., 2005).

The valley slopes show several different gravitational features that can schematically be grouped in two main types, (1) a "landslides zone", which is located at the toe of the slopes between the valley floor and the mid-slope, and (2) a "sackung zone", located between the mid-slope elevation and the mountain crest (Fig. 1). In the "landslides zone", toppling occurs in metamorphic rocks and affected by about 29 landslides with volumes ranging between 5 and 50×10^6 m^3. This zone contains some active large landslides, like the "La Clapière" landslide, which is located less than 1 km downstream from the Saint-Etienne de Tinée village (Cappa et al., 2004; Guglielmi et al., 2005). The "sackung zone" is characterized by extensional deformation structures, notably large tension cracks which are several kilometres in length and downhill-facing scarps up to several metres high. These landforms involve displacements along penetrative pre-existing joints and along newly-formed, metre-wide tension cracks. Gravitational features of the sackung zone extend deep inside the slope (Fig. 1).

The gravitational deformation history of the Tinée valley from 20 kyr to the present-day has been determined using ^{10}Be and ^{14}C dating methods, and geomorphologic analysis (see details in Bigot-Cormier et al. (2005)). The valleys of the massif were covered by glacier ice, 17 kyr ago. The glacier terminus was located at Isola village (elevation 900 m) and retreated to Saint-Etienne de Tinée (elevation 1100 m) at about 15 kyr ago. The main glacier in the Tinée valley disappeared around 13 kyr ago, and the first gravitational movements are dated at about 13–13.5 kyr. They correspond to the large landslides located around Isola. These landslides could have been triggered by stress release of the slope related to loss from the glacier ice. Subsequent slope failures are spread over time, with at least three stages: (1) 10–6 kyr BP and (2) 3–1 kyr BP, manifested by opening of cracks in mid- and upper slope positions, (3) and, historic major landslides at the toe of the slopes. No major climatic or tectonic events are associated with the instabilities. "The climatic optimum", which occurred around 6000 years and which can be considered as the only known major event that occurred in the area since 13 kyr ago involved no major change in precipitation rates that could have affected the slope stability through groundwater pressure increases (Bigot-Cormier et al., 2005). In conclusion, it is reasonable to consider that the large gravitational deformations that lasted for at least 13 kyr in the Argentera–Mercantour massif, some of them still currently very active, were not triggered by major catastrophic events. In the historical period, this was observed when the current La Clapière landslide was triggered close to the town of Saint-Etienne de Tinée (Fig. 1) in the early 1930s without any major precipitation event or earthquake being registered in the area (Follacci, 1987).

3. Detailed analysis of the La Clapière hillslope-scale progressive failure evolution

3.1. Spatial distribution of rock-slope deformations

At the toe of the La Clapière slope, a large active landslide affects the metamorphic Hercynian basement (Bogdanoff, 1986) made of gneisses and migmatites. The foliation planes are N120–130° oriented dipping 80° to the East. The slope is intensely cut at all scales by three families of inherited tectonic faults: N010°–030°, N090°, and N120°–140°.

The landslide activity is continuously monitored with electronic distance-metres (French Ministry of Equipment), and GPS (GeoAzur laboratory) and it has been extensively characterized through structural, mechanical and hydrogeological studies (Follacci, 1987;

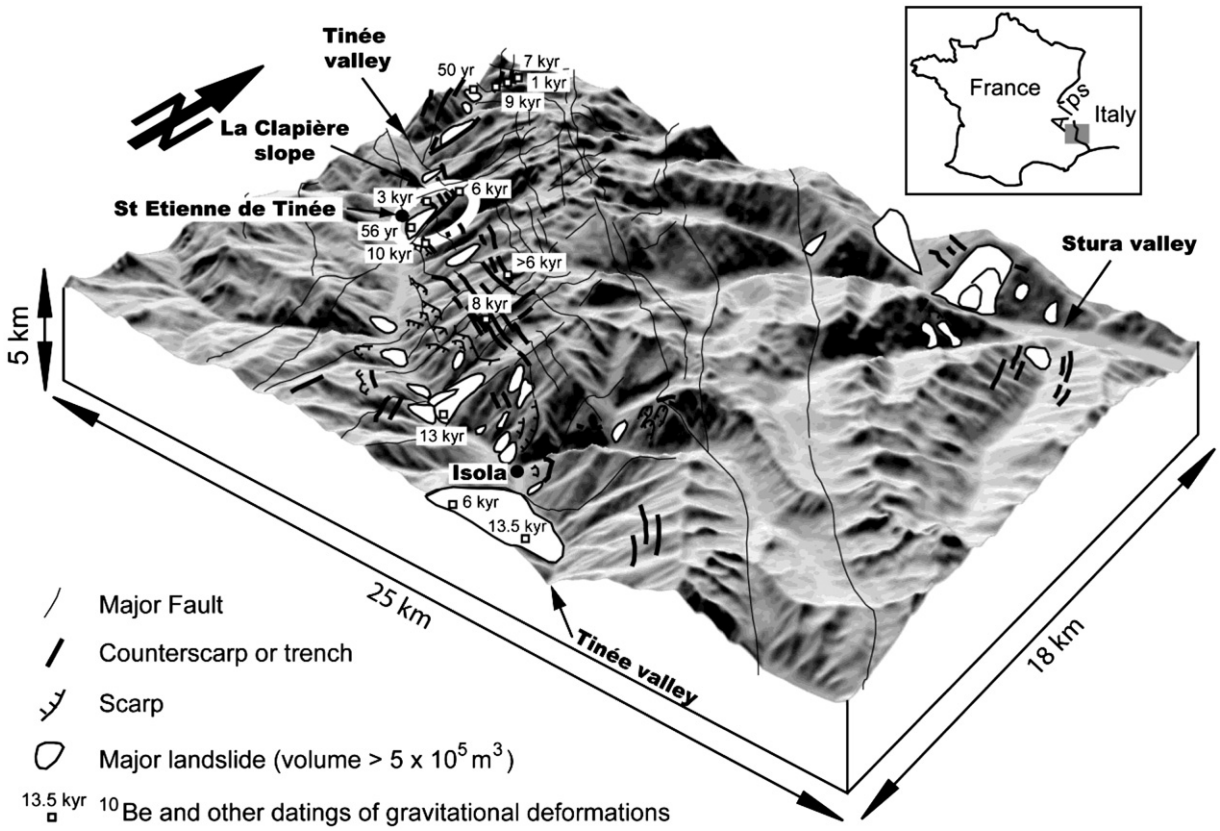

Fig. 1. 3D view showing fault zones and gravitational structures in the Argentera–Mercantour massif. The white circle near Saint-Etienne de Tinée gives the location of the La Clapière unstable slope.

Cappa et al., 2004; Guglielmi et al., 2005), and electrical tomography (Lebourg et al., 2005). The landslide activity was described since the early 1930s with a peak evolution between 1960 and 1990. From 1960 to 1990, the slope morphology was extremely deformed, with a 130 m high scarp that appeared in the middle of the slope. The active landslide estimated volume is 60×10^6 m^3. It is embedded in the remaining middle and upper parts of the slope that, although currently inactive, display deformation trench-like features that extend widely laterally and towards the slope crest. Twenty four trenches with an average orientation of N120° and lengths of 100 to 5000 m were mapped (Fig. 2). Trenches result either from the failure of the shallow part of major pre-existing fault zones or from a newly-formed failure related to the connection of minor pre-existing heterogeneities of the slope. The aperture of the trenches varies from 1 to 5.5 m. There is no significant lateral variation of the aperture within a single trench. The vertical offset is as small as few tens of centimetres in all cases (El Bedoui et al., 2009). The depth of the trenches varies from 10 to 50 m. Many trenches are filled with colluviums. The average trench orientation is parallel to the slope direction (Fig. 2). Trenches, which are closest to the currently active landslide main scarp, are highly rotated, and even cut by the scarp, while torsion becomes moderate in trenches located at mid-slope, above the landslide scarp, and non-existent in trenches far from the active landslide.

3.2. Chronology of La Clapière rock-slope deformations

A relative chronology of deformations can be established from the above-mentioned data. The active landslide cuts the trenches observed in the slope. This proves that the trenches appeared before the landslide. Secondly, trenches are deformed close to the landslide which proves that such rotation effect was induced by a higher deformation localized in the bottom southeastern part of the slope and that this deformation preceded the landslide. Thus, at least three deformation stages can be defined: (1) trenches opening, (2) trenches rotation, and (3) landslide triggering.

A detailed dating of the opening of trenches at different elevations in the slope and of the main scarp of the La Clapière active rock slide was conducted with ^{10}Be (for details see Bigot-Cormier et al. (2005)). Trenches appear progressively younger from the lower portion (10 kyr BP), the mid-portion (7.2 kyr BP) to the top (5.6 kyr BP) of the slope, meaning that there was a propagation of slope deformation from the toe to the top in about 4400 years. The upper lateral scarp of the currently active landslide was dated at 3.067 kyr BP, showing that after the upslope propagation of the deformation, a deep shear plane occurred in the middle part of the slope and bounded the currently active landslide.

4. Geomechanical model of progressive rock-slope failure

4.1. Conceptual model of progressive failure of the La Clapière slope

Taking the example of the La Clapière landslide, a conceptual model of the progressive failure at the scale of the slope was developed by El Bedoui et al. (2009) and is extended in the present study (Fig. 2). From 10 to 5 kyr BP (Fig. 2a–c), mainly trenches and a few scarps spread from the toe to the top of the slope. From 5 to 3.6 kyr BP (Fig. 2d), the trenches in the lower eastern part of the slope became rotated and displayed a large vertical displacement. A major failure occurred in the lower eastern part of the slope at about 3.067 kyr BP (Fig. 2d), and during the last 50 years this failure has enlarged and bounded the currently active La Clapière landslide (Fig. 2e). The current slope deformation is large and diffused, and regressive from 1600 to 2200 m in elevation. It is mainly characterized by horizontal displacement along the slope, and

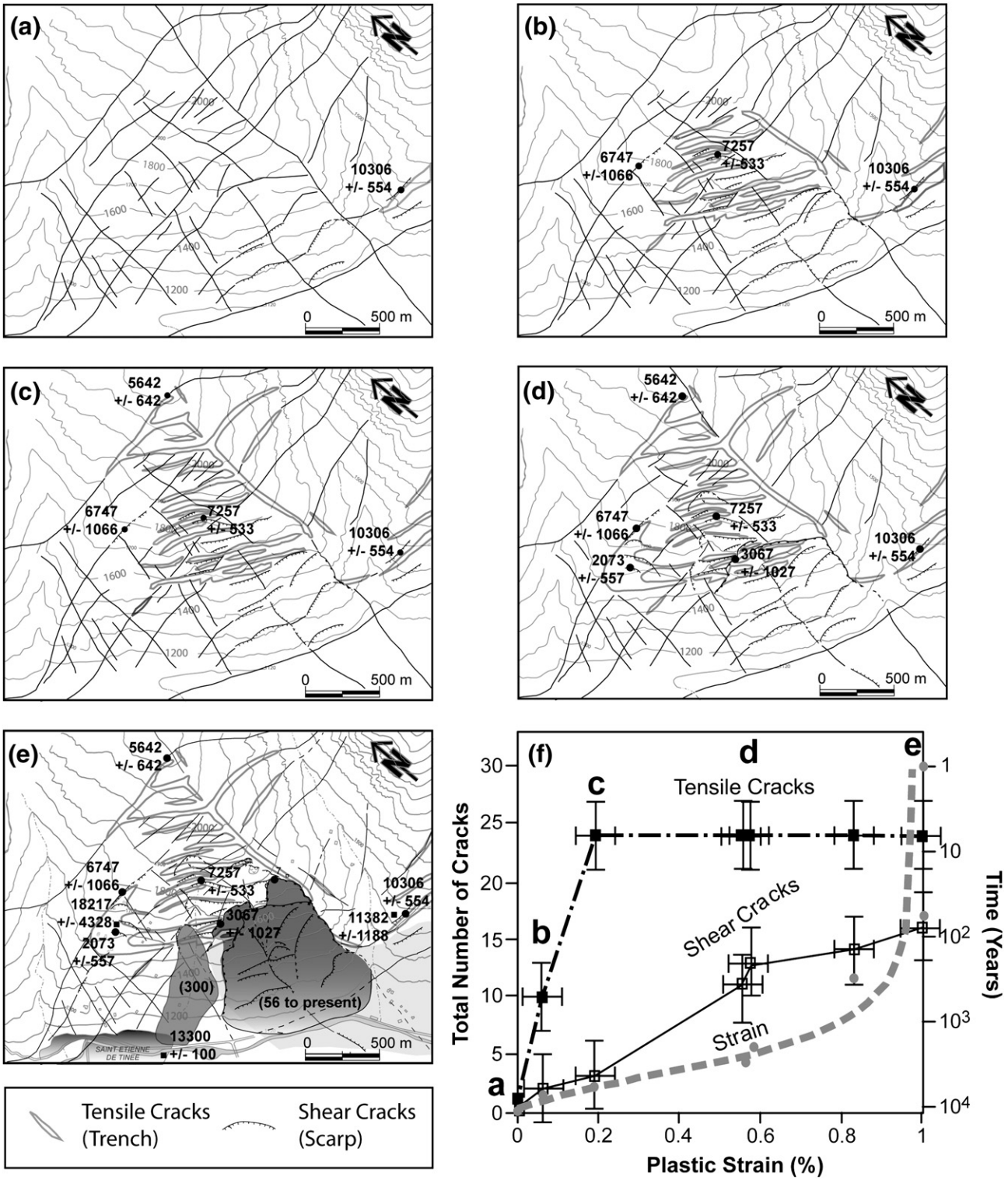

Fig. 2. Evolution of the La Clapière rock-slope deformations over the past 10 kyr (phases (a) to (e); dating are expressed in year), and (f) interpretation of crack evolution as function of plastic strain, and plastic strain as function of time (grey dashed line).

mainly localized in the basal slope. It also includes displacements with a vertical component related to a deep failure surface.

The conceptual rock-slope failure model relates trench and scarp openings in the past to the current La Clapière landslide at the slope toe (Fig. 2). Trench and scarp morphology are a good indicators of surface slope plastic deformations at the mountainous scale and for a long period of several thousand years. If we consider these trenches and scarps as tensile and shear cracks, respectively, we can use our morphostructural characterization and dating to semi-quantitatively estimate the evolution of the number of tensile and shear cracks with plastic strain and time (Fig. 2f). Indeed, El Bedoui et al. (2009) estimated the average slope displacement at six time intervals using ^{10}Be dates and measuring trench apertures and scarps offsets in the field. Six paleo-slope two-dimensional topographies were reconstructed after closing of the trenches and the scarps. The plastic strain was considered as the ratio of one given average paleo-slope

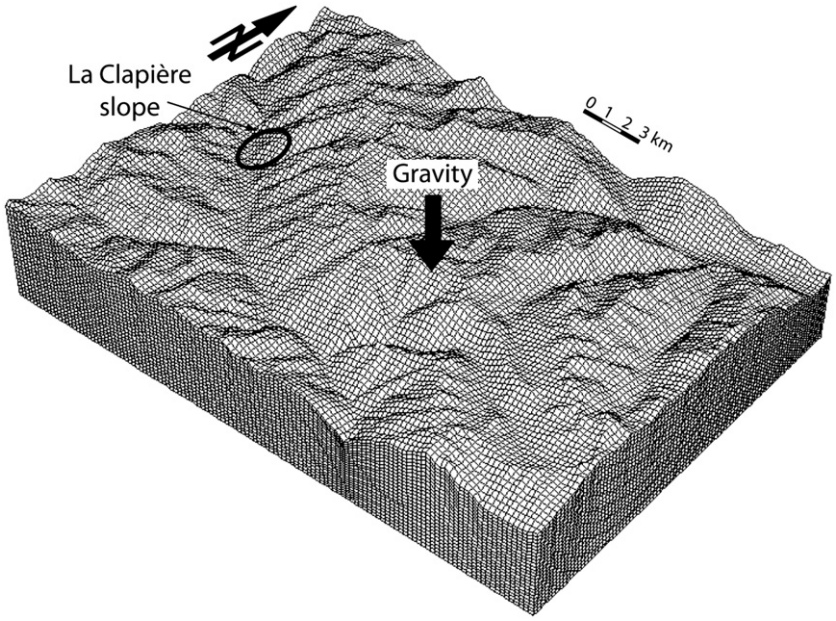

Fig. 3. Geometry of the numerical model with the location of the currently active La Clapière slope.

displacement-versus-the initial slope dimensions. Initial slope corresponds to the slope before any observed gravitational deformations which was reconstructed after closing all trenches and scarps. There has been a non-linear increase of tensile and shear cracks with plastic strain since 10 kyr. The number of tensile cracks increases strongly from phases (a) to (c), and remains constant until phase (e), whereas the number of shear cracks increases progressively from phases (a) to (e). This crack development results in a non-linear increase in plastic strain with time that indicates a progressive failure development through the rock-slope.

4.2. Extrapolation to the regional-scale analysis through numerical simulations

From the conceptual model mentioned above (Section 4.1), we analyzed the development of rock-slope failure at the regional-scale using numerical simulations. We developed a finite-difference model based on the FLAC^{3D} code (Itasca Consulting Group, 2006), assuming a 3D representation ($25\times18\times5$ km) of the topographic surface of the Argentera–Mercantour massif with extension to 5 km-depth in the shallow crust (Fig. 3). Model boundaries were restricted to the area where slope movements were analyzed in-situ in our study. In the model, each mesh element has a spatial resolution of 50 m. For simplicity, a homogeneous medium without faults is simulated. We considered the topography at the end of the last glaciation, 13 kyr ago, to be the "pre-failure" topography. To build this initial topography, we have smoothed the current topography (derived from the DEM with a spatial resolution of 10 m) removing slope movements. In the model, in-situ stresses were assumed, with a horizontal to vertical ratio of 0.686. This ratio was inferred from the complete stress determined using the "Hydraulic Tests on Pre-existing Fractures" method of Cornet et al. (1997). The topographic surface is free to move in the model, whereas no displacements were allowed normal to the bottom boundary and the natural stress gradient was set to the lateral boundaries. Elastic–plastic properties of intact (i.e., undisturbed) rock have been previously determined from laboratory and field data (Cappa et al., 2004) (Table 1). Failure occurs in the model when the shear stress acting in the rock exceeds its shear strength, approximated by a Coulomb criterion with tension cut-off:

$$\tau = c + \mu_s \sigma_n \quad (1)$$

where τ is the critical shear stress for failure, c is apparent cohesion, μ_s is the static friction coefficient, and σ_n is the normal stress. Assuming a composite Griffith–Coulomb failure envelope, the mode of rock failure is dependent on the differential stress $(\sigma_1-\sigma_3)$, and failure can occur in (Fig. 4) (Jaeger and Cook, 1979):

- shear if differential stress is relatively high: $(\sigma_1-\sigma_3)>6T$, where T is tensile strength (Fig. 4a);
- tension if differential stress is relatively low: $(\sigma_1-\sigma_3)<4T$ (Fig. 4c), and;
- hybrid tension/shear if differential stress is intermediate: $4T<(\sigma_1-\sigma_3)<6T$ (Fig. 4b).

During the simulations, gravity was applied until mechanical forces reached equilibrium. We consider this loading procedure to be representative of the deglaciation effect, which is rapid compared to the long period of time considered in this study. The model was initially elastically equilibrated under the gravity force. After this, failure initiation was analyzed for two cases, one with an elasto-plastic behaviour neglecting the effect of strength loss, and one with a cohesion weakening–frictional strengthening (CWFS) behaviour simulating the effect of strength loss (i.e. material degradation) (Fig. 5). In other words, the elasto-plastic model includes the effects of plastic straining and related stress redistribution on the depth of failure, but the material weakening is ignored. In this case, cohesion, friction and tensile strength are constant. The CWFS model (Hajiabdolmajid et al., 2002; Hajiabdolmajid and Kaiser, 2003; Hajiabdolmajid et al., 2003) was used with strength parameters

Table 1
Material properties.

Parameters	Rock	Plastic strain*
Young's modulus, GPa	60	
Poisson's ratio	0.3	
Density, kg/m^3	2500	
Initial friction angle, °	5	
Residual friction angle, °	40	0.2%
Initial cohesion, MPa	10	
Residual cohesion, MPa	0.1	0.6%
Initial tensile strength, MPa	4	
Residual tensile strength, MPa	0	0.25%

*Required plastic strain to reach the residual values in the CWFS model.

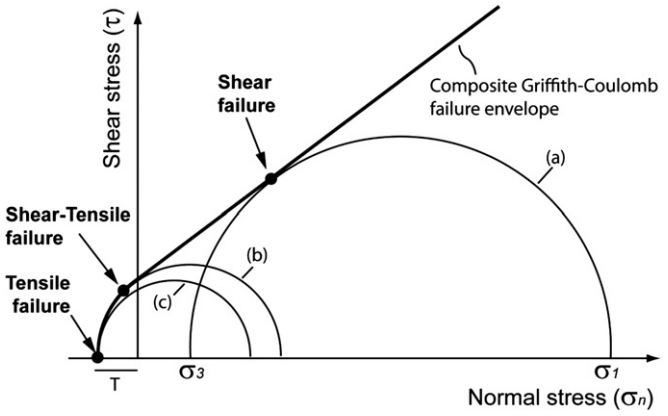

Fig. 4. Schematic Mohr diagram with composite failure envelope for intact rock with tensile strength (T), illustrating the stress conditions for: (a) shear failure (higher differential stress, $\sigma_1-\sigma_3$); (b) hybrid tension/shear failure; and, (c) tensile failure (lower differential stress).

(Fig. 6a–b) set to a coherent rock mass and then automatically modified, with the strength progressively decreasing as a function of increasing plastic strain. This model comparison allows us to investigate the effects of strength degradation on the development of slope failures.

4.3. Modelling results

4.3.1. Elasto-plastic model neglecting the effect of strength loss

Results indicate that some slopes become unstable, experiencing tensile and shear failure, when the rocks are assigned values of cohesion of 10 MPa, a friction of 5° and a tensile strength of 4 MPa (Fig. 6c). These values appear reasonable for intact rocks with low confinement levels like those studied. For instance, a laboratory testing of late alpine gneiss yields a value of cohesion of 16 MPa for intact rock and a value of few tens of kPa for damaged rock (Willenberg, 2004; Gunzburger et al., 2005). Eberhardt et al. (2005) have also used similar parameters to analyze failure of gneisses involved in the Randa rockslide in Swiss Alps. The elasto-plastic behaviour used in the model includes the effects of plastic straining and related stress redistribution at the depth of failure, and ignores rock weakening; it therefore provides an upper limit for failure occurrence and consequently for values of cohesion, friction and tensile strength. In this model, failure zones are mainly located in the downstream locations of the Tinée and Stura valleys. Shear failures are initiated at the transition of the steep rock slopes to the valley floor, whereas few tensile failures appear at mid-slope positions.

4.3.2. Cohesion weakening–frictional strengthening (CWFS) model

Results presented in Fig. 6d to f show a progressive failure sequence, with a transition from stable slope zones to those of damage. The progressive failure can be viewed as strength degradation in the form of shear and tensile failure development. Simulations indicate that failure occurs and evolves with a low reduction in cohesion (loss of 0.4 MPa), tensile strength (loss of 0.2 MPa) and an increase in friction from 5° to 8°. As the model reaches equilibrium, the maximum state of material damage corresponds to a plastic shear strain of 0.34% and a plastic tensile strain of 0.16%. From onset to steady-state, rock-slope failures develop and propagate on each side of the Tinée valley, in the adjacent small valleys, and in the Stura valley (Fig. 6d–e). Shear failures are located mainly at the toe of the slopes, while several zones of tensile failure form just above those of shear failure mid-slope positions. This result is in good accordance with the gravitational deformations observed in the field, as shown in Fig. 7 for the case of the La Clapière slope. Failure spreads in two ways: (1) from the downstream to upstream portions of the valleys, and (2) from the toe to mid-slope positions. At the slope-scale, failure initiates through shearing of the rocks at the toe of the slope, which allows kinematic release and development of tensile failures at the mid-slope. Accumulation of damage ultimately leads to dramatic failure. This failure sequence is in agreement with conventional theory in which shear stresses are localized at the base of the steep rock slopes and provide a source for initiation of progressive shear failure, in combination with tensile stresses at mid- and upper slope locations, which induce tensile failures oriented sub-parallel to the slope.

5. Discussion

5.1. Accuracy and limits of validity of the model

Our simulations allow an analysis of progressive failure sequences in slopes at the regional-scale. There is a good correspondence between the location of simulated shear and tensile failure zones and the landslides and sackung zones observed in the field (Figs. 1 and 6).

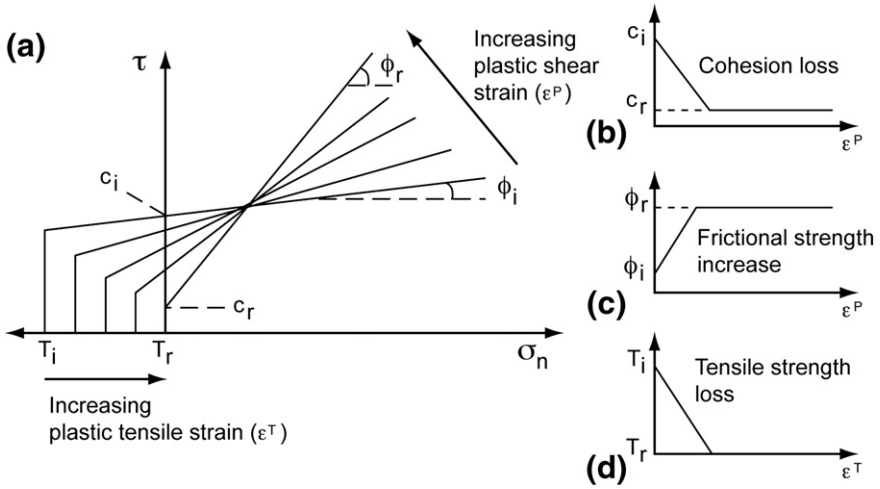

Fig. 5. Illustration of the CWFS model with (a) sequential failure envelopes in a shear stress-versus-normal stress diagram showing the transition from mostly cohesive to almost exclusively frictional yield mode; and, mobilization of (b) cohesion, (c) frictional strength and (d) tensile strength as a function of plastic strain. The CWFS model introduced by Hajiabdolmajid et al. (2002) produces the evolution of the failure envelope, such that at low confinement, the cohesive strength initially predominates the mobilized strength, and it eventually is replaced by the frictional strength when the cohesion is consumed. The model can capture both the initiation and the arrest of rock failure.

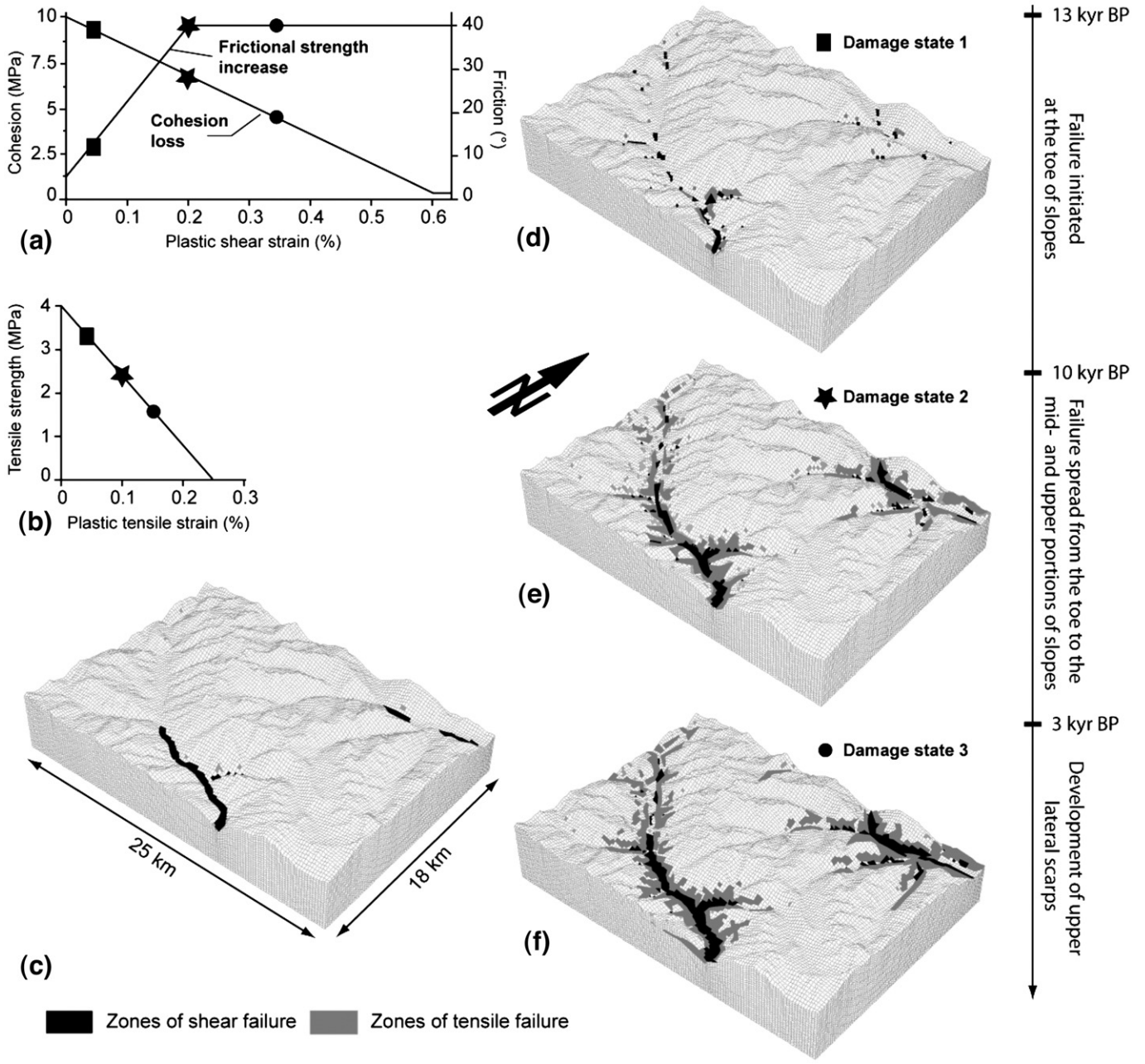

Fig. 6. (a) Cohesion loss and increase in the frictional strength as a function of plastic shear strain; (b) Decrease in tensile strength as a function of plastic tensile strain; (c) Failure simulated with an elasto-plastic model neglecting the effect of rock strength loss; (d) to (f) Incremental shear and tensile failure over three damage stages simulated with a cohesion weakening–frictional strengthening (CWFS) model.

In detail, the model slightly underestimates the extension of the failure zone towards the mountain crest, probably because the rock mass is represented as a homogeneous medium. The slope is cut by pre-existing faults, which act as weak zones that become partly reactivated by gravitational movements, complicating the sequential deformation of the slope (Guglielmi et al., 2005; Hippolyte et al., 2006). In addition to the effect of weak fault zones, a certain degree of anisotropy in the intact strength of the gneiss could also affect the deformations. The tensile and shear nature of the failure as indicated in our study conducted at the scale of a mountainous region therefore supports the strain-dependent strength development concept used by Hajiabdolmajid and Kaiser (2002), and Eberhardt et al. (2001), to analyze the initiation and progressive failure at the smaller scale of rock slopes at the Frank and Randa slides, respectively.

5.2. Factors of dramatic to more gradual time evolution

The first simulated failures appear mainly at downstream locations (Fig. 6d) and may explain the 13 kyr old landslides, near Isola in the Tinée valley (Fig. 1). Simulated failures then spread upstream and from the toe upward in the slopes. The failures depicted in Fig. 6e correspond to the 10 to 3 kyr old deformation shown in Fig. 1. The last simulated shear failures, which appear in Fig. 6f, correspond to the 20th century, and still active, landslides (Fig. 1). The simulated gravitational failure sequence proves that (1) the loss of rock strength related to damage is about 13 kyr in duration in the case of fractured gneissic rocks of the Argentera–Mercantour massif, and (2) zones of active landsliding evolve and their locations strongly depend on this long progressive failure sequence.

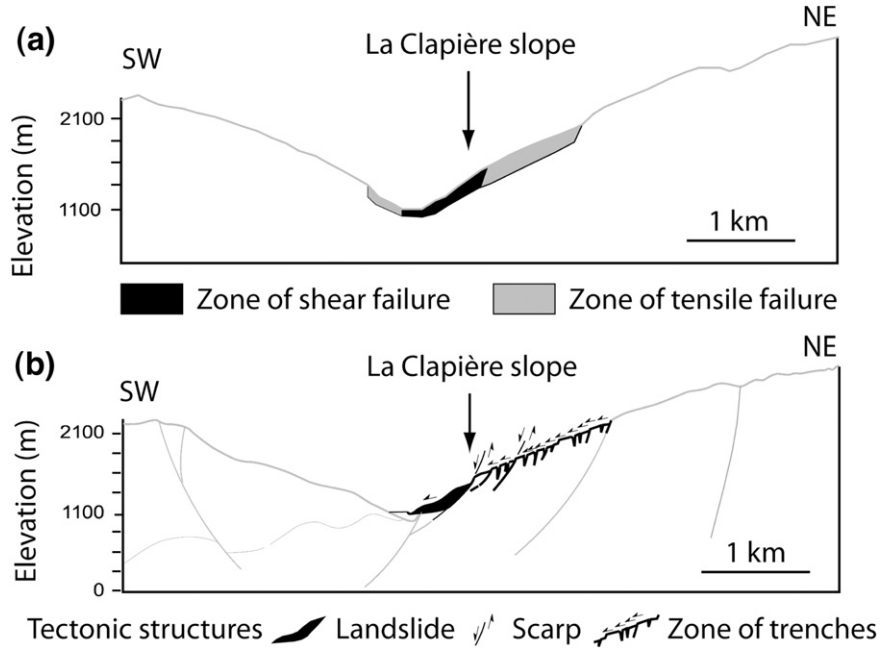

Fig. 7. Comparison of (a) zones of shear and tensile failure simulated using the CWFS model, with (b) the gravitational deformations observed in the case of the La Clapière slope.

6. Conclusion

We combine a three-dimensional, numerical, geomechanical analysis and regional-scale field mapping and dating of gravitational movements to show how the strength of shallow rocks decreases over long periods of time. In the Argentera–Mercantour case study, this approach shows that the stress change accompanying terminal Pleistocene deglaciation is sufficient to initiate an extended loss of strength in the shallow crust, leading to a sequence of deep-seated gravitational deformation, the latest of which is historic rockslides. This process probably operates in all formerly glaciated regions where two main types of gravitational deformations coexist: (1) large deep-seated deformation, characterized by "sackung", and (2) much smaller, catastrophic landslides (Kinakin and Stead, 2005). Our research shows the possible link between these two types of mass movements, and also shows that deglaciation may play a key role in damage of shallow crustal rocks.

Acknowledgments

This work has been supported by the GIS CURARE research project. The authors are grateful for the constructive comments and recommendations by the associate editor, Takashi Oguchi, and an external technical review by Jia-Jyun dong at the National Central University, Taiwan, and one unidentified reviewer, which substantially improved this paper.

References

Agliardi, F., Crosta, G., Zanchi, A., 2001. Structural constraints on deep-seated slope deformation kinematics. Eng. Geol. 59, 83–102.
Amitrano, D., 2003. Brittle–ductile transition and associated seismicity: experimental and numerical studies and relationship with the *b* value. J. Geophys. Res. 108 (B1), 2044. doi:10.1029/2011JB000680.
Bachmann, D., Bouissou, S., Chemenda, A., 2004. Influence of weathering and preexisting large scale fractures on gravitational slope failure: insights from 3-D physical modelling. Nat. Hazards Earth Syst. Sci. 4, 711–717.
Bachmann, D., Bouissou, S., Chemenda, A., 2006. Influence of large scale topography on gravitational rock mass movements: new insights from physical modeling. Geophys. Res. Lett. 33, L21406. doi:10.1029/2006GL028028.
Bachmann, D., Bouissou, S., Chemenda, A., 2008. Analysis of massif fracturing during Deep Seated Gravitational Slope Deformation by physical and numerical modelling. Geomorphology. doi:10.1016/j.geomorph.2007.09.018.
Ballantyne, C.K., 2002. Paraglacial geomorphology. Quat. Sci. Rev. 21, 1935–2017.
Bigot-Cormier, F., Braucher, R., Bourlès, D., Guglielmi, Y., Dubar, M., Stéphan, J.F., 2005. Chronological constraints on processes leading to large active landslides. Earth Planet. Sci. Lett. 235, 141–150.
Bogdanoff, S., 1986. Evolution de la partie occidentale du massif cristallin externe de l'Argentera. Place dans l'arc alpin. Geol. France 4, 433–453.
Brückl, E., Parotidis, M., 2005. Prediction of slope instabilities due to deep-seated gravitational creep. Nat. Hazards Earth Syst. Sci. 5, 155–172.
Cappa, F., Guglielmi, Y., Merrien-Soukatchoff, V., Mudry, J., Bertrand, C., Charmoille, A., 2004. Hydrochemical modeling of a large moving rock slope interred from slope levelling coupled to spring long-term hydrochemical monitoring: example of the La Clapière landslide (Southern Alps, France). J. Hydrol. 291, 67–90.
Chemenda, A., Bouissou, S., Bachmann, D., 2005. 3-D Physical Modeling of Deep-Seated Landslides: new technique and first results. J. Geophys. Res. 110, F04004. doi:10.1029/2004JF000264.
Cornet, F.H., Wileveau, Y., Bert, B., Darcy, J., 1997. Complete stress determination with the HTPF tool in mountainous region. Int. J. Rock Mech. Min. Sci. 34 (3–4) Paper No.057.
Diederichs, M.S., 1999. Instability of hard rockmasses: the role of tensile damage and relaxation. PhD thesis, Department of Civil Engineering, University of Waterloo, Waterloo, Canada, 566 pp.
Dramis, F., Sorriso-Valvo, M., 1994. Deep-seated gravitational slope deformations, related landslides and tectonics. Eng. Geol. 38, 231–243.
Eberhardt, E., Stead, D., Stimpson, B., 1999. Quantifying progressive pre-peak brittle fracture damage in rock during uniaxial compression. Int. J. Rock Mech. Min. Sci. 36 (3), 361–380.
Eberhardt, E., Willenberg, H., Loew, S., Maurer, H., 2001. Active rockslides in Switzerland—understanding mechanisms and processes. International Conference on Landslides—Causes, Impacts and Countermeasures, Davos, pp. 25–34.
Eberhardt, E., Stead, D., Coggan, J.S., 2005. Numerical analysis of initiation and progressive failure in natural rock slopes—the 1991 Randa rockslide. Int. J. Rock. Mech. Min. Sci. 41, 69–87.
El Bedoui, S., Guglielmi, Y., Lebourg, T., Perez, J.L., 2009. Deep-seated failure propagation in a fractured rock slope over 10,000 years: the La Clapière slope, the south-eastern French Alps. Geomorphology 105, 232–238.
Follacci, J.P., 1987. Les mouvements du versant de la Clapière à Saint-Etienne-de-Tinée (Alpes-Maritimes). Bull. Lab. Ponts Chaussées 150–151, 107–109.
Guglielmi, Y., Cappa, F., Binet, S., Bigot-Cormier, F., Tric, E., 2004. Multi-scale rock slope failure initiation mechanisms: results from multi-parametric field and modeling studies conducted on the Upper Tinée Valley (French Alps) over the past 10 years. Proceedings of the GeoHazards - 2004 Workshop, Shizuoka, Japan, pp. 100–104.
Guglielmi, Y., Cappa, F., Binet, S., 2005. Coupling between hydrogeology and deformation of mountainous rock slopes: insights from La Clapiere area (southern Alps, France). C. R. Geosciences 337, 1154–1163.
Gunzburger, Y., Merrien-Soukatchoff, V., Guglielmi, Y., 2005. Influence of daily surface temperature fluctuations on rock slope stability: case study of the Rochers de Valabres slope (France). Int. J. Rock Mech. 42, 331–349.
Hajiabdolmajid, V., Kaiser, P.K., 2002. Slope stability assessment in strain-sensitive rocks. Eurock 02, Proceedings of the ISRM International Symposium on Rock Engineering in Mountainous Regions, Funchal, Madeira, pp. 237–244.
Hajiabdolmajid, V., Kaiser, P.K., 2003. Brittleness of rock and stability assessment in hard rock tunneling. Tunn. Undergr. Space Technol. 18, 35–48.

Hajiabdolmajid, V., Kaiser, P.K., Martin, C.D., 2002. Modeling brittle failure of rock. Int. J. Rock Mech. Min. Sci. 39, 731–741.
Hajiabdolmajid, V., Kaiser, P.K., Martin, C.D., 2003. Mobilised strength components in brittle failure of rock. Géotechnique 53 (3), 327–336.
Hippolyte, J.C., Brocard, G., Tardy, M., Nicoud, G., Bourlès, D., Braucher, R., Ménard, G., Souffaché, B., 2006. The recent fault scarps of the Western Alps (France): tectonic surface ruptures or gravitational sackung scarps? A combined mapping, geomorphic, levelling, and ^{10}Be dating approach. Tectonophysics 418 (3–4), 255–276.
Itasca Consulting Group, 2006. FLAC^{3D}, Fast Lagrangian Analysis of Continua in 3 Dimensions, Version 2.0. Five volumes, Minneapolis, Minnesota, Itasca Consulting Group.
Jaeger, J.C., Cook, N.G.W., 1979. Fundamentals of Rocks Mechanics, 3rd ed. Chapman & Hall, London. 480 p.
Jarman, D., 2006. Large rock slope failures in the Highlands of Scotland: characterisation, causes and spatial distribution. Eng. Geol. 83, 161–182.
Kemeny, J., 2003. The time-dependent reduction of sliding cohesion due to rock bridges along discontinuities: a fracture mechanics approach. Rock Mech. Rock Eng. 36 (1), 27–38. doi:10.1007/s00603-002-0032-2.
Kemeny, J., 2005. Time-dependent drift degradation due to the progressive failure of rock bridges along discontinuities. Int. J. Rock Mech. Min. Sci. 42, 35–36.
Kinakin, D., Stead, D., 2005. Analysis of the distributions of stress in natural ridge forms: implications for the deformation mechanisms of rock slopes and the formation of sacking. Geomorphology 65 (1–2), 85–100.
Lebourg, T., Binet, S., Tric, E., Jomard, H., El Bedoui, S., 2005. Geophysical survey to estimate the 3D sliding surface and the 4D evolution of the water pressure on part of a deep seated landslide. Terra Nova 17, 399–406.
Martin, C.D., Chandler, N.A., 1994. The progressive fracture of Lac du Bonnet granite. Int. J. Rock Mech. Min. Sci. Geomech. Abstr. 31 (6), 643–659.
Martin, C.D., Kaiser, P.K., McCreath, D.R., 1999. Hoek–Brown parameters for predicting the depth of brittle failure around tunnels. Can. Geotech. J. 36 (1), 136–151.
Mogi, K., 1966. Pressure dependence of rock strength and transition from brittle fracture to ductile flow. Bull. Earthquake Res. Inst. (Japan) 44, 215–232.
Petley, D.N., Mantovani, F., Bulmer, M.H., Zannoni, A., 2005. The use of surface monitoring data for the interpretation of landslide movement patterns. Geomorphology 66, 133–147.
Willenberg, H., 2004. Geologic and kinematic model of a complex landslide in crystalline rock (Randa, Switzerland), Ph.D Thesis, Swiss Federal Institute of Technology, Zurich, 161 pp.
Zischinsky, U., 1966. On the deformation of high slopes. Proceedings, 1st International Conference International Society for Rock Mechanics, Lisbon, vol. 2, pp. 179–185.